Evaluation of the Performance of the Water Cloud Model and Modified Water Cloud Model in estimating Soil Moisture: a Case Study of Kiruuli Village

Mark Mukomazi Buyungo[1], Ivan Bamweyana[1,2]
[1] Department of Geomatics and Land Management, Makerere University, Kampala-Uganda
[2] ivanson5@gmail.com

DOI: https://dx.doi.org/10.4314/sajg.v13i1.2

Abstract

In Uganda, crop yields have been constrained by recurrent droughts and reliance on rain-fed agriculture. As a straightforward measure, irrigation farming has been adopted by the government through its rehabilitation of old schemes and its assistance to farmers in the setting up of micro-irrigation farms. Of consequence is the fact that the maximization of crop yields through irrigation necessitates soil moisture data for irrigation scheduling. Both ground-based measurements and remote sensing techniques can be used to access this information, with the latter holding the advantage of gathering more information over a wider area. Because of its ability to account for vegetation cover, the Water Cloud Model (WCM) ─ a remote sensing-based model ─ has been widely used in earlier studies to estimate soil moisture content over vegetated areas. However, the accuracy of the model is limited by the assumption that vegetation is a homogenous scatterer. Thus, the Modified Water Cloud Model (MWCM) was developed in accordance with the debate that by considering the heterogeneous scattering nature of the vegetation, it would perform better than the WCM. Using Kiruuli Village (in a coffee-growing area), this study compared the performance of the WCM and the Modified Water Cloud Model (MWCM) in estimating soil moisture. The models were implemented using Sentinel 1 and 2 images acquired on 05 September 2021 and 02 August 2021, respectively. Results showed that the MWCM performed slightly better than the WCM with Root Mean Square Errors (RMSEs) of 3.3346 and 3.7482, respectively. The marginality of the results can be attributed to a relatively high vegetation fraction at the time of image acquisition and a reasonably small area of comparison. Generally, more work can be carried out to compare the models across a larger area with a sparser vegetation cover.

Key Words: *soil moisture, remote sensing, Modified Water Cloud Model (MWCM)*

1. Introduction

Soil moisture contributes about 0.001% to the total volume of water found on Earth and plays a significant role in regulating plant growth, weather and climate (European Space Agency,

2021). This is because it is an interface of energy interactions between the land and atmosphere that acts as a variable in various processes on the soil surface such as evaporation, infiltration and runoff (Ezzahar *et al.*, 2020).

Amongst its other applications in agriculture, soil moisture is an important variable for the determination of the optimal sowing date and for scheduling irrigation inputs. In the field of agriculture, soil moisture plays a vital role in different processes and activities, such as, amongst others, the determination of the optimal sowing date and the scheduling of irrigation inputs. Irrigation-based agriculture constitutes 20% of the total cultivated land and 40% of the total food produced worldwide (World Bank, 2020). Because of the increase in the world population, urbanization and climate change, the struggle for water resources is expected to increase globally and will in the future impact agriculture and food availability.

In Uganda, the water supply for agricultural activities conducted in terms of a subsistence approach is primarily rain-fed. Because of changes in rainfall patterns and the subsequently prolonged dry spells, soil moisture deficits occur at times that may be extremely important for plant growth (Sundin and Lindbald, 2015; Wanyama *et al.*, 2017). This limits the crop yields attained by farmers. According to the World Bank, (2020), irrigated agriculture is on average at least twice as productive per unit of land as rain-fed agriculture. To boost the productivity of the country's agricultural sector, the backbone of the economic sector, the Ugandan government operates through various players, amongst others, the Ministry of Agriculture, Animal Industry and Fisheries (MAAIF), Ministry of Water and Environment (MWE), Ministry of Energy and Mineral Development (MEMD). Furthermore, the Uganda National Planning Authority (2020) is carrying out irrigation developments through the rehabilitation of the existing irrigation schemes and by offering assistance to local farmers in the setting up of mini-irrigation schemes. The success of these developments will depend on several factors, including amongst others, the efficient scheduling of irrigation programmes. Since this developmental issue necessitates soil moisture data, it is crucial to accurately monitor this variable over time.

Soil moisture data can be obtained through field measurements. However, these are costly, time-consuming and inefficient in the case of large farming areas where information pertaining to soil moisture varies spatially. Several remote sensing approaches provide soil moisture information over large areas and on a continuous basis. For example, Abdulrahamani's (2019) study to assess the WCM's capability to estimate soil moisture over the Kakira sugar plantation proved successful. However, its accuracy is limited owing to the assumption it makes that the vegetation canopy is a homogeneous scatterer. In a bid to mitigate this issue, Zhang et al., (2021) developed the Modified Water Cloud Model, which introduces the vegetation fraction parameter to account for the uneven distribution of vegetation. Whereas a previous study carried out by Zhang

et al., (2021) assessed both models using Radarsat-2 and Landsat-8 imagery over wheatfields, this study looked at using Sentinel imagery which has a higher temporal resolution (six days) in comparison to that used by Radarsat (24 days) and Landsat (16 days). The methodology to remove the effect of vegetation on the measured Synthetic Aperture Radar (SAR) backscatter requires the use of a cloud-free optical image captured on the same date as that captured by the SAR image. In practice though, there is always a risk of cloud cover when it comes to optical images. When such an issue is encountered, it has proved to be more beneficial in cases where less time is needed for the next image to be produced, the objective being to facilitate an estimation of the soil moisture content. Therefore, this study aimed to evaluate the performance of the WCM and MWCM in estimating soil moisture using Sentinel image data across a coffee-growing area.

This paper is arranged as follows: In section 2, the study area, data and steps taken to obtain results are described. Section 3 expounds on the models. Section 4 presents the results and discussions. Finally, section 5 rounds up the discussion with conclusions and recommendations.

2. Study area, data and methods

Kiruuli Village (the study area) is located between $0°45.55'S$ and $0°47.06'S$ latitudes and $31°27.86'E -$ and $31°29.23'E$ longitudes in Kisaasa parish, Kifamba sub-county, Kakuuto county, Rakai district, Uganda. The village has an area of about four square kilometres (4 km^2), which is relatively small compared to the 270 km^2 site investigated by Zhang et al. (2021). A vast part of the land is used for coffee cultivation. The western part of the village, mainly a hilly area, is characterized by grassland vegetation and rocky soils, whereas the central and eastern parts are lowlands, with arable soils. Figure 2.1 shows the location of Kiruuli village and its location in Rakai district. The coffee growing area was chosen because coffee is, amongst others, the country's leading exported crop and because the coffee plant grows in combination with the sparse natural vegetation cover. The latter fact served to make the comparison of the two models as an effective tool in the context of this research.

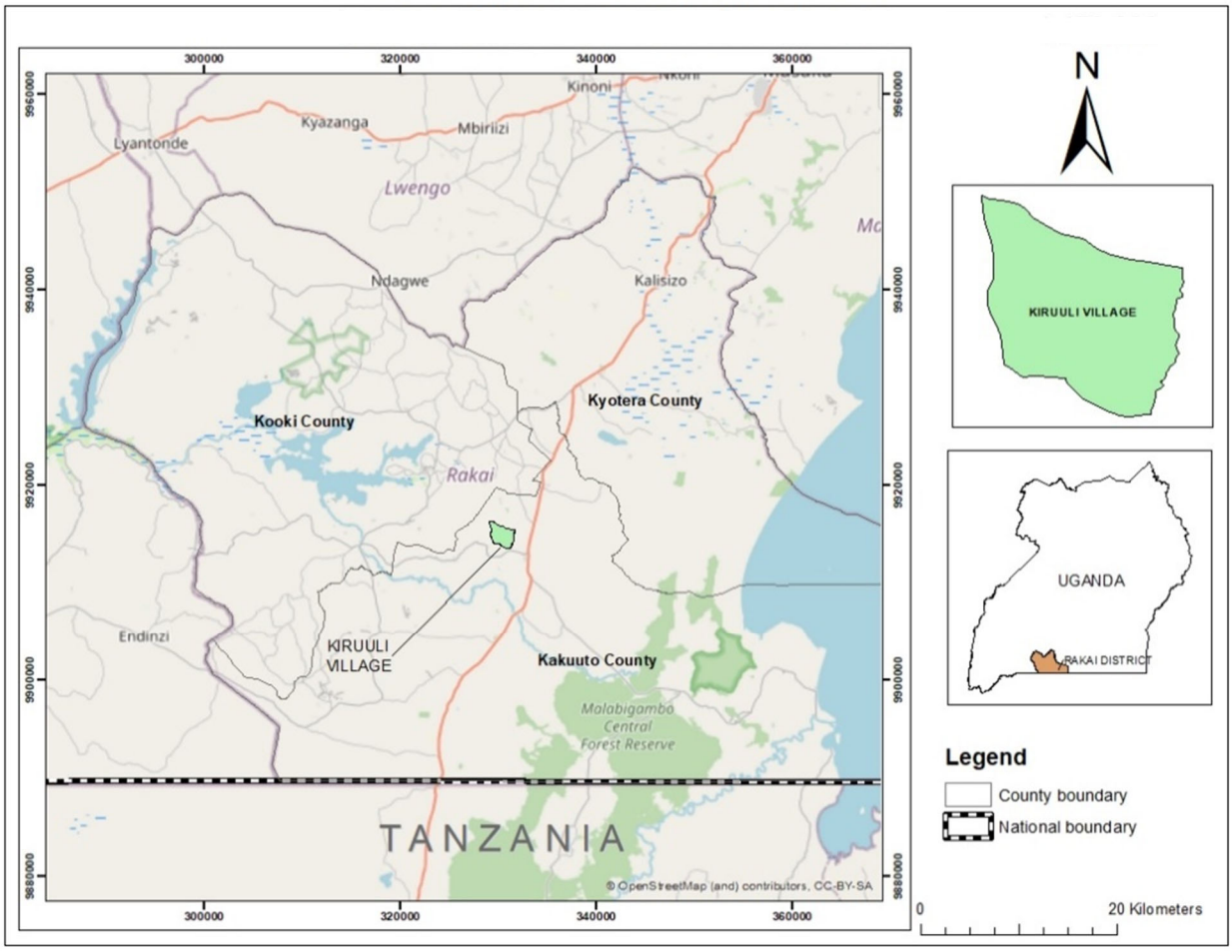

Figure 2.1: Location of Kiruuli village

2.1. In-situ data

Soil samples were obtained randomly from different coffee-growing locations within the study area and by using a metal core ring, at a depth of five centimetres (5 cm). For each location ─ as determined by using a handheld GPS instrument ─, three samples were collected within a buffer zone of five metres (5m). The soil samples were placed in zipping bags and then transported to the laboratory for the computation of their soil moisture content. A total of 16 locations (plots) were sampled, 10 of which were of the vegetated area and six of bare soil (Refer to figure 2.2).

2.2 Imagery

Sentinel-1 is a satellite Synthetic Aperture Radar (SAR) mission launched by the European Space Agency (ESA). It involves a constellation of two satellites launched at different times ─ that is in 2013 and 2016 ─, and results in Sentinel-1a and Sentinel-1b images, respectively (Davids and Rouyet, 2018). It offers SAR data in the C band at a temporal resolution of six days and supports both co-polarization and cross-polarization. Vertical transmit-Vertical receive (VV) polarization was used since it is more sensitive to soil moisture than Vertical transmit-Horizontal receive (VH)

polarization in vegetated areas. This is due to the high sensitivity to the volumetric scattering of the latter (Baghdadi *et al.*, 2017; Gao *et al.*, 2017). An IW GRDH (Interferometric Wide Ground Range Detected, High Resolution) image corresponding to the same date (05 September 2021) as that of the *in-situ* data was downloaded from the Copernicus open access hub and used for this study.

Sentinel-2 is an optical, wide swathe, high-resolution multispectral imaging mission involving two satellites, namely Sentinel-2A and Sentinel-2B, launched in June 2015 and in March 2017, respectively (Gao *et al.*, 2017). It was developed for land monitoring studies (SNAP - ESA Sentinel Application Platform V8.0.0, no date). It consists of 13 multispectral bands, four of which are of a 10-metre spatial resolution, six of 20 metres and three of 60 metres. A Sentinel-2 MSIL2A (Multi-Spectral Imager Level 2A) image acquired on 02 August 2021 was downloaded from the Copernicus open access hub and used for this purpose; the assumption was that the vegetation cover had not changed significantly within the 33-day interval. An image for the same date as that for the *in-situ* data and even those closer than the one deployed could not be used as a result of the dense cloud cover.

2.2. Data processing

Generally, the methodology is shown in Figure 2.3, where the Sentinel-1 image was subset to reduce its size for faster processing. The image subset was preprocessed through steps described by Filipponi, (2019). These include the following: the application of an orbit file, thermal noise removal, border noise removal, calibration, speckle filtering, geometric correction and conversion to decibels.

As with the Sentinel-1 image, the Sentinel-2 image was initially a subset. The image subset was then resampled to resize the pixels of all the image bands to a 10-metre resolution. The resampled product was masked using a shapefile of the study area to generate the area of interest. The masked product was reprojected to match the same coordinate system as the Sentinel-1 image. From the reprojected product, the different vegetation descriptors were processed; they were CWC, LAI, f_{veg} and m_{veg}. The resultant bands were collocated to the Sentinel-1 backscatter (dB) image. Using the bare soil backscatter and the measured soil moisture, bare soil parameters C and D were obtained by means of linear regression. They were resampled to resize the pixels of all the image bands to a 10-metre resolution. The resampled product was masked by using a shapefile of the study area to generate the area of interest. The masked product was reprojected to match the same coordinate system as the Sentinel-1 image. From the reprojected product, the different vegetation

descriptors, namely, CWC, LAI, f_{veg} and m_{veg}., were processed. The resultant bands were collocated to the Sentinel-1 backscatter (dB) image. Using the bare soil backscatter and the measured soil moisture, bare soil parameters C and D were obtained through linear regression. Based on a study carried out by Bindlish and Barros (2001) that obtained vegetation constants A and B over different underlying surfaces, values of 0.0018 and 0.138 which correspond to the crop area were used for the two constants, respectively. The radar incidence angle over the study site was in the region of 38^0. With all the necessary parameters, equations 6 and 9 were regarded as inputs in the band maths tool in SNAP and the soil moisture products were generated. These were used to generate the distribution of the estimated soil moisture in the study area (Refer to figure 4.2). Statistical metrics used in the analysis included the Pearson rank coefficient (r) and the Root Mean Square Error (RMSE) Where r indicates the strength of the linear relationship between the two variables from a range of -1 to 1. The closer the r value approaches ± 1, irrespective of the direction, the stronger the current relationship, thus conveying a greater linear relationship between the two variables. On the other hand, RMSE is a metric that serves to summarize the errors in the prediction of a given variable into a single value. It is obtained from the formula

$$RMSE = \sqrt{\frac{1}{n}\left(\sum_{i=1}^{n} e_i^2\right)} \tag{10}$$

where: i represents an index, n is the number of observations and e_i is the error in the i^{th} observation.

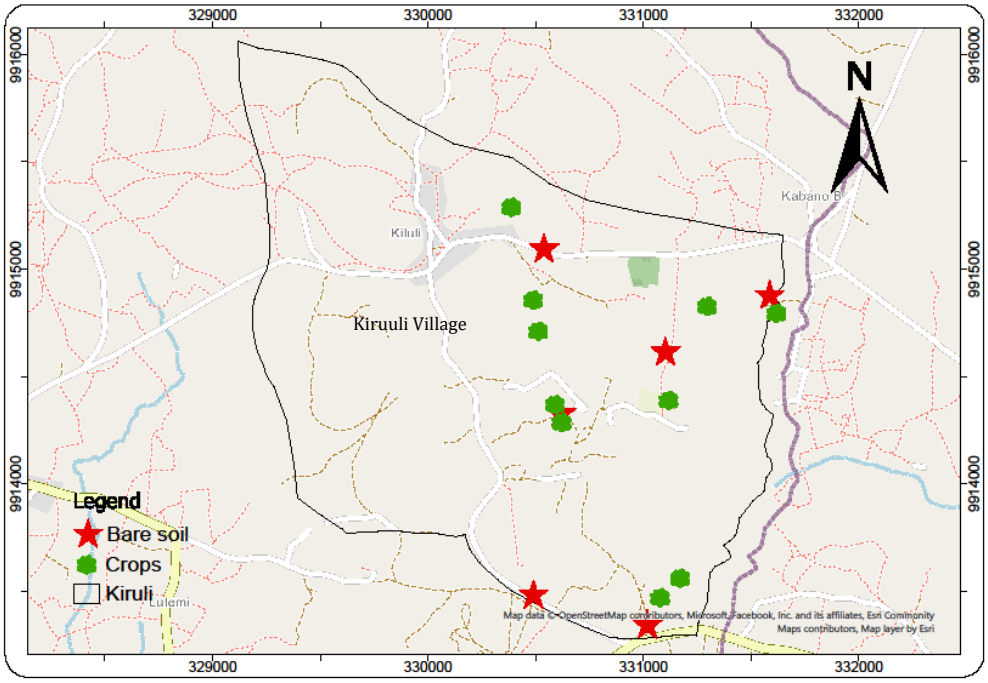

Figure 2.2: The distribution of *in-situ* data points in the study area

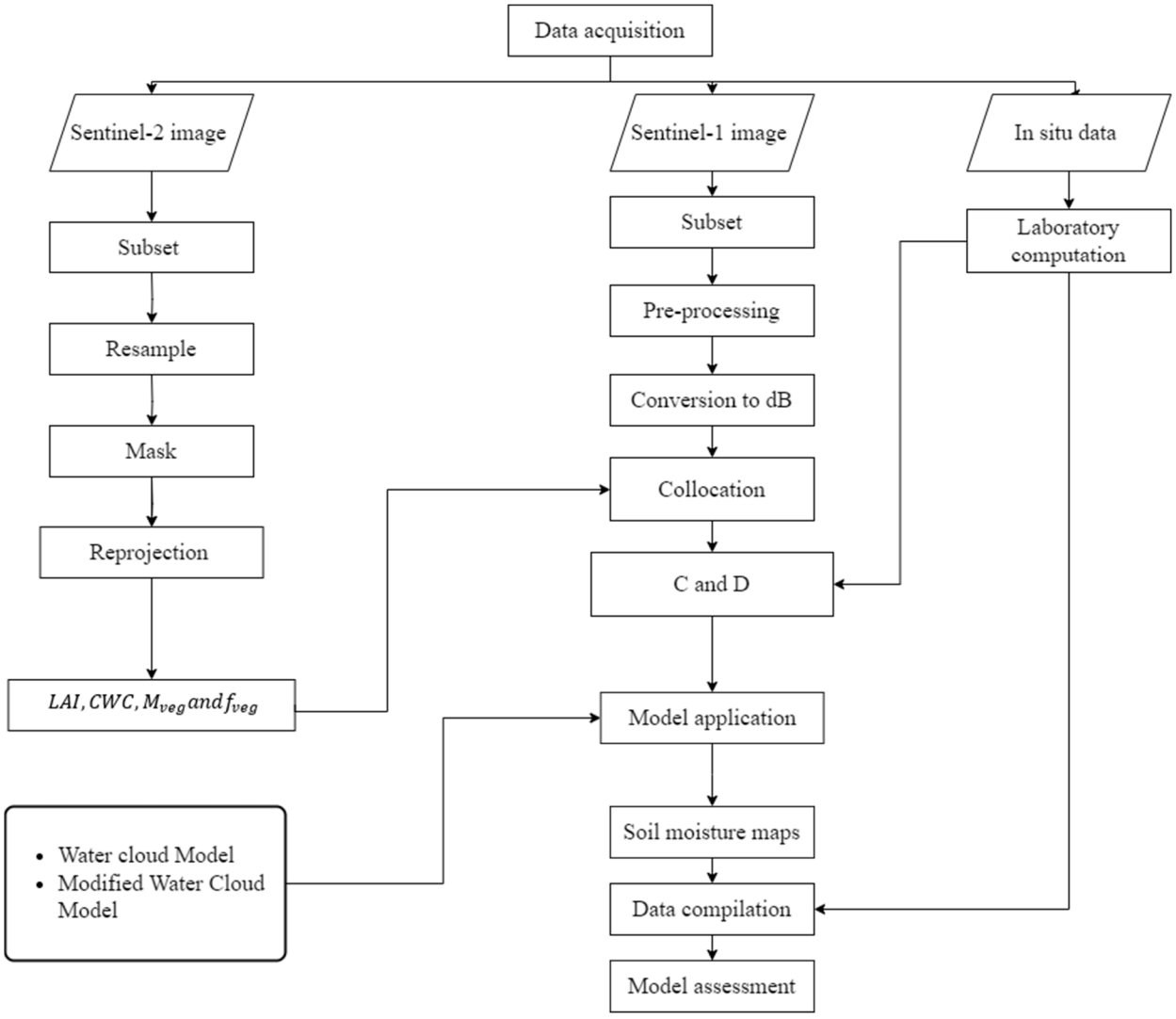

Figure 2.3: Methodology

3. Model descriptions

The Water Cloud Model, designed by Attema and Ulaby (1978), is effective in estimating soil moisture over vegetated areas. This is due to its ability to account for the contribution of vegetation to the total SAR backscatter in terms of the following relationship:

$$\sigma^{\circ}_{pp} = \sigma^{\circ}_{veg} + \sigma^{\circ}_{veg+soil} + L^2\sigma^{\circ}_{soil} \quad (1)$$

where $\sigma^{\circ}_{pp} = \sigma^{\circ}_{veg} + \sigma^{\circ}_{veg+soil} + L^2\sigma^{\circ}_{soil}$ is the co-polarized total backscatter coefficient, $\sigma^{\circ}_{pp} = \sigma^{\circ}_{veg} + \sigma^{\circ}_{veg+soil} + L^2\sigma^{\circ}_{soil}$ is the backscatter contribution of the vegetation cover, $\sigma^{\circ}_{pp} = \sigma^{\circ}_{veg} + \sigma^{\circ}_{veg+soil} + L^2\sigma^{\circ}_{soil}$ is the multiple scattering involving vegetation elements and the soil surface, $\sigma^{\circ}_{pp} = \sigma^{\circ}_{veg} + \sigma^{\circ}_{veg+soil} + L^2\sigma^{\circ}_{soil}$ is the backscatter contribution of the soil surface, and L^2 is the two-way vegetation attenuation.

The second term is considered insignificant in co-polarized radiation and often neglected (Kumar et al., 2012; Baghdadi *et al.*, 2017; Ayehu *et al.*, 2020). Hence,

$$\sigma^{\circ}_{pp} = \sigma^{\circ}_{veg} + L^2\sigma^{\circ}_{soil} \quad (2)$$

with

$$\sigma^{\circ}_{veg} = AV_1 cos\theta(1 - L^2) \quad (3)$$

$$L^2 = exp(-2BV_2 sec\theta) \quad (4)$$

$$\sigma^{\circ}_{soil} = C + DM_v \quad (5)$$

where V_1 and V_2 are vegetation descriptors. This research used Leaf Area Index (LAI) as V_1 and Canopy Water Content (CWC) as V_2 for the WCM (Kumar et al., 2012). The symbol, θ, is the radar incidence angle; A and B are the vegetation parameters, with A representing the albedo of the vegetation and B representing the attenuation factor; C and D correspond to the bare soil parameters obtained through linear model fitting; and M_v represents the volumetric soil moisture.

Making soil moisture the subject and substituting σ°_{veg}, L^2 and σ°_{soil} in equation 2 results in

$$M_v = \frac{1}{D}\left[\frac{\sigma^{\circ}_{pp} - AV_1 Cos\theta(1-\exp(-2BV_2 sec\theta))}{exp(-2BV_2 sec\theta)} - C\right] \quad (6)$$

Unlike the WCM, which assumes vegetation as a homogeneous scatterer (Attema and Ulaby, 1978; Ayehu *et al.*, 2020; Zhang et al., 2021), the MWCM incorporates the vegetation fraction parameter to account for the uneven distribution of vegetation. This is more representative of the vegetation characteristics of an area, especially a sparsely vegetated area (Zhang et al., 2021). The MWCM developed by Zhang et al. (2021) is expressed as follows:

$$\sigma^{\circ}_{pp} = f_{veg}\left(\sigma^{\circ}_{veg} + L^2\sigma^{\circ}_{soil}\right) + (1 - f_{veg})\sigma^{\circ}_{soil} \quad (7)$$

where

$$f_{veg} = \frac{NDVI - NDVI_{soil}}{NDVI_{veg} - NDVI_{soil}} \quad (8)$$

Making soil moisture the subject and substituting σ°_{veg}, L^2 and σ°_{soil} in equation 7, gives:

$$M_v = \frac{1}{D}\left[\frac{\sigma^{\circ}_{pp} - f_{veg} m_{veg} Cos\theta(1-\exp(-2Bm_{veg} sec\theta))}{(f_{veg} exp(-2Bm_{veg} sec\theta) + 1 - f_{veg})} - C\right] \quad (9)$$

4. Results and discussion

4.1. In-situ data

Table 4.1 presents the soil moisture content of the various soil samples obtained using the thermo-gravimetric method, also known as the oven-drying method. The volumetric soil moisture values ranged from 4.7115 to 11.6559 cm^3, showing a low soil moisture content across the area. This was an actual depiction of the dry conditions that persisted until October when heavy rains were experienced across the study area, and no irrigation activities were observed.

Table 4.1: In-situ data

Feature ID	X (m)	Y (m)	Feature	Gravimetric soil moisture (% of weight)	Oven-dry bulk density (g/ cm^3)	Volumetric soil moisture (% vol.)
1	331508.232	9915175.490	Bare soil	8.8077	1.3234	11.6559
2	331023.932	9914911.391	Bare soil	8.0927	1.3333	10.7898
3	330940.020	9913640.039	Bare soil	7.4290	1.3497	10.0270
4	330411.721	9913780.713	Bare soil	7.4454	1.5085	11.2313
5	330538.749	9914625.065	Bare soil	7.8988	1.4676	11.5923
6	330460.452	9915391.502	Bare soil	8.3716	1.3447	11.2569
7	331538.204	9915088.704	Crops	5.5523	1.4949	8.3000
8	331216.636	9915120.987	Crops	5.8688	1.3969	8.1982
9	331037.259	9914682.739	Crops	4.2567	1.2624	5.3737
10	331090.425	9913854.375	Crops	6.6835	1.2319	8.2337
11	330998.076	9913763.344	Crops	3.4953	1.3480	4.7115
12	330541.437	9914578.737	Crops	5.1555	1.3792	7.1103
13	330511.132	9914663.533	Crops	7.0206	1.1976	8.4080
14	330432.541	9915004.832	Crops	6.9977	1.1498	8.0461
15	330409.783	9915149.890	Crops	5.4290	1.2724	6.9080
16	330307.675	9915581.959	Crops	9.0306	0.9698	8.7579

4.2. Validation of models

The fitted models were validated by examining the agreement between the estimated backscatter and the observed backscatter. Results revealed that the WCM produced an R^2 of

0.6063, whereas the MWCM produced an R^2 value of 0.6115. The model fitting was considered good, with an R^2 value of 0.5 used as the threshold.

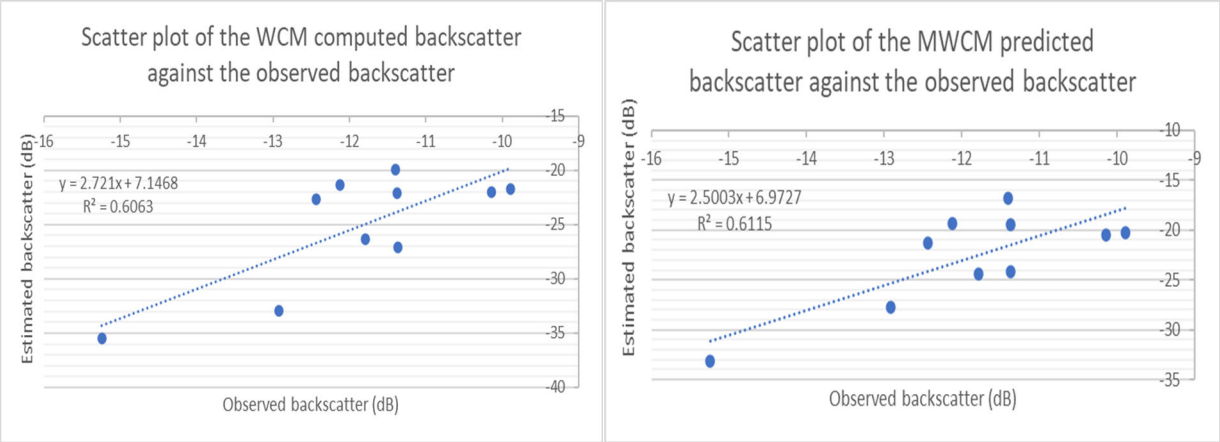

Figure 4.1: Scatter plots showing the relationship between predicted backscatter and observed backscatter: left (WCM); right (MWCM).

From Figure 4.2, it can be seen that the soil moisture content of the WCM was higher than that of the MWCM at similar locations. Further analysis pertaining to Figure 4.3 revealed that this was because the soil moisture values for WCM were overestimated and more than those for the MWCM. In addition, the two maps generally reflected a lower soil moisture content on the western side of the village which could be attributed to the rocky nature of the soils in the hilly portion of the village in contrast to the mainly sandy soils in the lowlying areas (central and eastern portions of the village).

Figure 4.3 clearly shows that the models overestimated the volumetric soil moisture content with the overestimation in the case of the MWCM being less than that for the WCM. A significant error in the estimation of soil moisture was observed for some points (e.g., *in-situ* point 3). In a study by El Hajj et al. (2016), overestimation was determined for soil moisture values below 20 cm^3 which declined as the values increased. Underestimations were experienced beyond the 30 cm^3 values,. Figure 4.3 shows a similar trend where overestimation generally declined as the soil moisture content increased.

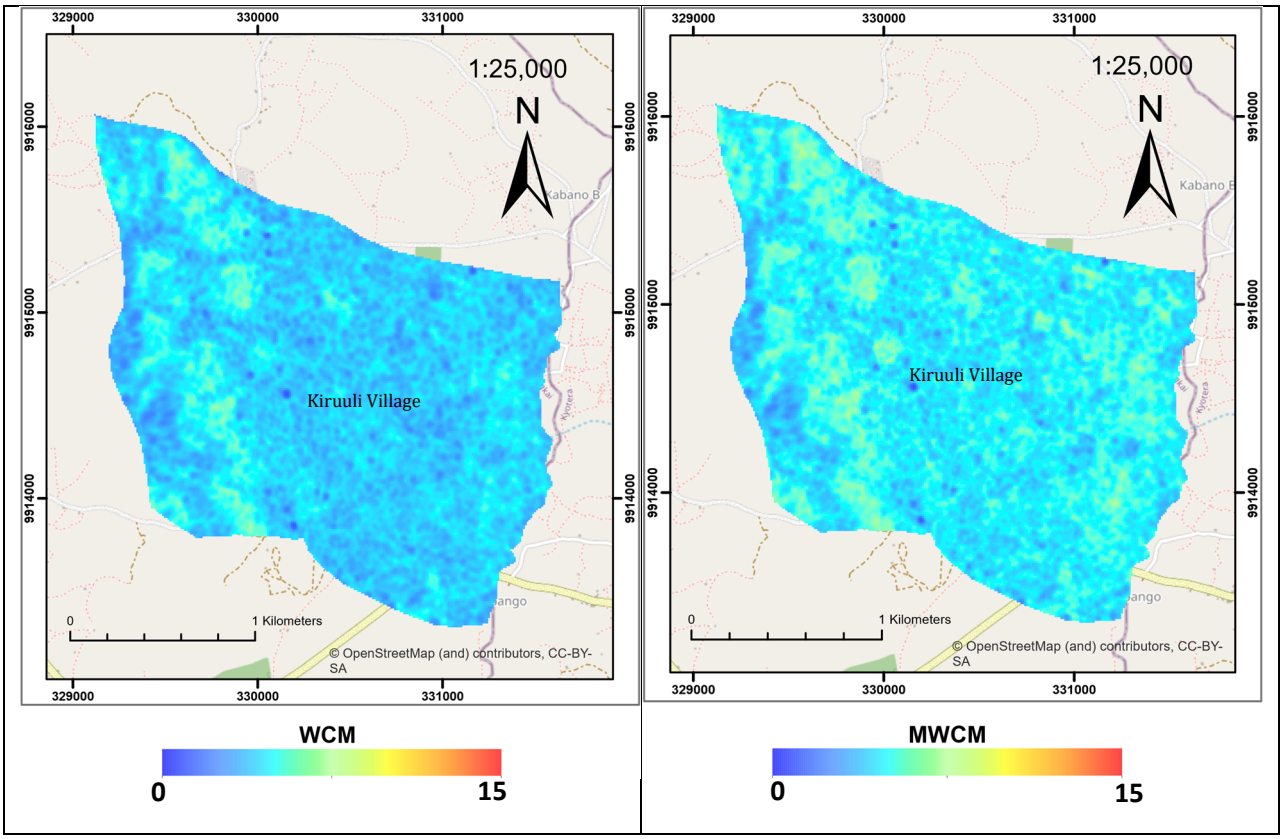

Figure 4.2: Maps showing the distribution of estimated soil moisture content

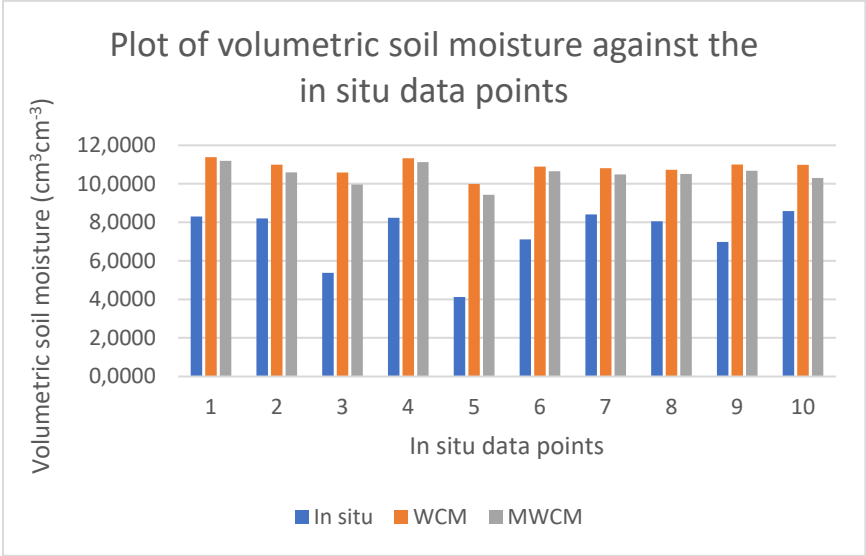

Figure 4.3: A plot of volumetric soil moisture content against the in-situ data points

Table 4.2: Statistical summary of results

Statistic	WCM	MWCM
R^2	0.6093	0.6175
R	0.7806	0.7858
RMSE	3.7482	3.3346

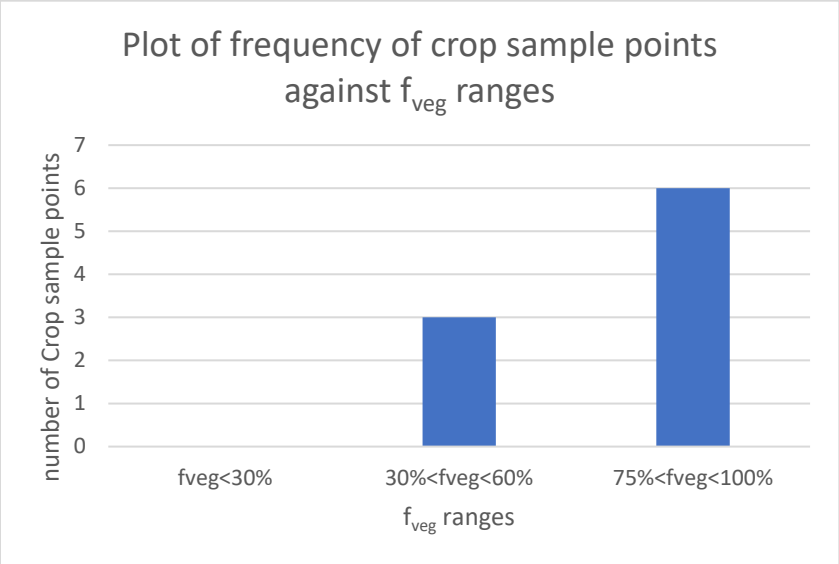

Figure 4.4: The number of crop soil samples in various vegetation fraction (fveg) ranges

A low RMSE, a high R^2 and a high r-value are indicative of a good model. Values in Table 4.2 show that the MWCM had a lower RMSE of 3.3346 and a higher r of 0.7858 compared to the WCM, with an RMSE of 3.7482 and an r-value of 0.7806. Based on this, the MWCM performed better than the WCM in terms of soil moisture estimation. However, a closer look at the values shows a slight difference between the performance of the two models. Further analysis of these results was carried out on the basis of figure 4.4. Figure 4.4 illustrates non-uniformity in the vegetation fraction at the different sampling points. This is so because coffee plants are grown by different farmers across the study area; thus, the coffee plants sampled in this research were not selected at the same growth stage. From figure 4.4, there were no crop soil samples that fell into the region of low vegetation fraction (f_{veg}<30%), three were in the medium vegetation fraction region (30%<f_{veg}<60%), six fell in the high vegetation fraction region (75%<f_{veg}<100%) and one fell between the medium and high vegetation fraction regions, namely, f_{veg} at ($f_{veg} = 66\%$). Generally, the data reflected different stages that were relatively high. The difference in performance, however, declined as the crop matured. Both models were close in their estimation

at the filling stage where there was a high vegetation fraction. With the situations in this study being largely similar , they could be the cause of the marginal difference. Furthermore, the small size of the area investigated could be a limiting factor leading to a greater variation in the set of results.

5. Conclusions and Recommendations

5.1. Conclusions

This study evaluated the performance of the WCM and MWCM in estimating soil moisture across a coffee-growing area. The assessment compared soil moisture estimated by the models using Sentinel-1 and Sentinel-2 data with *in-situ* data. With R^2 values of 0.6093 and 0.6175 and r values of 0.7806 and 0.7858, respectively, the results obtained showed the potential of both the MWCM and WCM to estimate soil moisture in the top five centimetres of the soil when the estimated soil moisture was plotted against the *in-situ* data. This study identified the MWCM as a better model for a coffee study site than the WCM. However, the difference in performance was not very significant owing to the relatively high vegetation fraction of the crops at the time of data capture.

5.2. Recommendations

The C-band (as offered by the Sentinel-1 mission) used in this study faces the challenge of penetrating dense vegetation, and this limits the accuracy with which soil moisture can be estimated. Hence, further research could be carried out to explore the L-band SAR data in estimating soil moisture. In addition, better accuracy would be achieved by incorporating surface roughness parameters which were omitted because the instruments used to measure them were unavailable.

The challenge of using a SAR image and an optical image on different dates to accommodate the issue of the cloud cover in the optical image had an impact on the derived WCM/MWCM parameters used to describe the vegetation characteristics of the given area. However, this could be mitigated by using the Simple Algorithm for Yield estimate (SAFY)model, which simulates the vegetation characteristics of a given area on the basis of meteorological data (Duchemin *et al.*, 2008; Han *et al.*, 2020). The absence of meteorological data hampered the use of the model in this research but future research could consider its application for better results when faced with a similar challenge.

In-situ data is a prerequisite for calibration and for assessing model accuracy. The *in-situ* data used in this research applied to one day only. Furthermore, the unavailability of data at various

crop growth stages limited a deeper evaluation of the models at such stages. The Ministry of Agriculture should, therefore, consider setting up various stations for soil moisture monitoring at the various irrigation schemes. This would make data available for the spatiotemporal evaluation of models and any further research on soil moisture.

6. Acknowledgement

The sincere appreciation of the authors is extended to the Hope Ministries company for the support it rendered in the collection of the *in-situ* data.

7. References

Abdulrahamani, A. (2019) *Estimation of Soil Moisture using Sentinel-1 and Sentinel-2 Satellite Data*. Makerere University.

Attema, E. P. W. and Ulaby, F. T. (1978) 'Vegetation modeled as a water cloud', *Radio Science*, 13(2), pp. 357–364.

Ayehu, G. *et al.* (2020) 'Combined Use of Sentinel-1 SAR and Landsat Sensors Products for Residual Soil Moisture Retrieval over Agricultural Fields in the Upper Blue Nile Basin, Ethiopia', *MDPI*, pp. 1–23.

Baghdadi, N. *et al.* (2017) 'Calibration of the Water Cloud Model at C-Band for Winter Crop Fields and Grasslands', *MDPI*, pp. 1–13. doi: 10.3390/rs9090969.

Bindlish, R. and Barros, A. P. (2001) 'Parameterization of vegetation backscatter in radar-based, soil moisture estimation', *Remote Sensing of Environment*, 76(1), pp. 130–137. doi: 10.1016/S0034-4257(00)00200-5.

Davids, C. and Rouyet, L. (2018) *Remote sensing for the mining industry*. Tromso.

Duchemin, B. *et al.* (2008) 'A simple algorithm for yield estimates: evaluation for semi-arid irrigated winter wheat monitored with green leaf area index', *Environmental Modelling and Software*, 23(7), pp. 876–892. doi: 10.1016/j.envsoft.2007.10.003.

European Space Agency (2021) *Nearly four decades of soil moisture data now available*. Available at: http://www.esa.int/Applications/Observing_the_Earth/Space_for_our_climate/Nearly_four_decades_of_soil_moisture_data_now_available (Accessed: 19 May 2021).

Ezzahar, J. *et al.* (2020) 'Evaluation of backscattering models and support vector machine for the retrieval of bare soil moisture from Sentinel-1 data', *Remote Sensing*, 12(1), pp. 1–20. doi: 10.3390/RS12010072.

Filipponi, F. (2019) 'Sentinel-1 GRD Preprocessing Workflow †', *MDPI*, pp. 1–4. doi: 10.3390/ECRS-3-06201.

Gao, Q. *et al.* (2017) 'Synergetic Use of Sentinel-1 and Sentinel-2 Data for Soil Moisture Mapping at 100 m Resolution'. doi: 10.3390/s17091966.

El Hajj, M. *et al.* (2016) 'Soil moisture retrieval over irrigated grassland using X-band SAR data', *Elsevier*, 176, pp. 202–218. doi: 10.1016/j.rse.2016.01.027.

Han, D. *et al.* (2020) 'Linking an agro-meteorological model and a water cloud model for estimating soilwater content over wheat fields'. *Computers and Electronics in Agriculture*, 179(17), p. 105833. doi: 10.1016/j.compag.2020.105833.

Kumar, K., Hari Prasad, K. S. and Arora, M. K. (2012) 'Estimation of water cloud model vegetation parameters using a genetic algorithm', *Hydrological Sciences Journal*, 57(4), pp. 776–789. doi: 10.1080/02626667.2012.678583.

SNAP - ESA Sentinel Application Platform V8.0.0 (no date) *No Title*. Available at: http://step.esa.int.

Sundin, C. and Lindbald, N. (2015) *Water and Agriculture in Uganda*.

Uganda National Planning Authority (2020) 'Third National Development Plan (NDPIII) 2020/21-2024/25', *National Planning Authority* (January), pp. 1–310. Available at: http://envalert.org/wp-content/uploads/2020/06/NDP-3-Finale.pdf.

Wanyama, J. *et al.* (2017) 'Irrigation Development in Uganda : Constraints , Lessons learned , and Future Perspectives', 143(1). doi: 10.1061/(ASCE)IR.1943-4774.0001159.

World Bank (2020) *Water in Agriculture*. Available at: https://www.worldbank.org/en/topic/water-in-agriculture (Accessed: 20 May 2020).

Zhang, M., Lang, F. and Zheng, N. (2021) 'Soil Moisture Retrieval during the Wheat Growth Cycle using SAR and Optical Satellite Data', *MDPI*, pp. 1–19.